Since January 2020 Elsevier has created a COVID-19 resource centre with free information in English and Mandarin on the novel coronavirus COVID-19. The COVID-19 resource centre is hosted on Elsevier Connect, the company's public news and information website.

Biochemical and Biophysical Research Communications 616 (2022) 14–18

Contents lists available at ScienceDirect

Biochemical and Biophysical Research Communications

journal homepage: www.elsevier.com/locate/ybbrc

Structural insights into ORF10 recognition by ZYG11B

Bing Zhang [a, 1], Yao Li [a, 1], Qiqi Feng [a], Lili Song [b], Cheng Dong [a, **], Xiaojie Yan [a, *]

[a] Department of Biochemistry and Molecular Biology, The Province and Ministry Co-sponsored Collaborative Innovation Center for Medical Epigenetics, Key Laboratory of Immune Microenvironment and Disease (Ministry of Education), School of Basic Medical Sciences, Tianjin Medical University, Tianjin, 300070, China

[b] Department of Immunology, The Province and Ministry Co-sponsored Collaborative Innovation Center for Medical Epigenetics, Key Laboratory of Immune Microenvironment and Disease (Ministry of Education), Tianjin Key Laboratory of Cellular and Molecular Immunology, School of Basic Medical Sciences, Tianjin Medical University, Tianjin, 300070, China

ARTICLE INFO

Article history:
Received 11 May 2022
Accepted 18 May 2022
Available online 20 May 2022

Keywords:
ORF10
ZYG11B
Cullin-RING E3 ligase
Crystal structure

ABSTRACT

Coronavirus disease 2019 (COVID-19) caused by severe acute respiratory syndrome coronavirus 2 (SARS-CoV-2), has become a major threat to human health. As a unique putative protein of SARS-CoV-2, the N-terminus of ORF10 can be recognized by ZYG11B, a substrate receptor of the Cullin 2-RING E3 ubiquitin ligase (CRL2). Here we elucidated recognition mechanism of ORF10 N-terminus by ZYG11B through presenting the crystal structure of ZYG11B bound to ORF10 N-terminal peptide. Our work expands the current understanding of ORF10 interaction with ZYG11B, and may also inspire the development of novel therapies for COVID-19.

1. Introduction

Coronavirus disease 2019 (COVID-19) caused by severe acute respiratory syndrome coronavirus 2 (SARS-CoV-2) has led to highly pathogenic diseases in humans, from common colds to acute respiratory distress syndrome and even death [1]. Because of its rapid spreading and high fatality, COVID-19 has become a big threat to human health [2]. Thus far, no effective treatment has been developed for this severe disease. Many researches explored the molecular details of pathogenesis of SARS-CoV-2 by genomics, transcriptomics, proteomics, and metabolomics technologies [3]. Previous studies have shown that although the genome of SARS-CoV-2 is very similar to SARS-CoV-1, there are some differences in their 3′ ORFs (open-reading frames): *ORF3b* and *ORF10* of SARS-CoV-2 are absent in SARS-CoV-1 [4], indicating the unique functional possibility of these two ORFs. *ORF10* encodes a putative 38-amino acid viral protein, and systematical protein-protein interaction studies confirmed the interaction between ORF10 protein of SARS-CoV-2 and human ZYG11B [5]. ZYG11B, as a substrate receptor of Cullin 2-RING E3 Ubiquitin ligase (CRL2), is able to specifically recognize N-terminal degradation signal starting with glycine in protein, termed Gly/N-degron, for ubiquitination and subsequent degradation by 26S proteasome [6]. Unexpectedly, Mena et al. found that ORF10 has no relevance to the E3 activity of ZYG11B and the interaction between them has no effect on SARS-CoV-2 infection in vitro [5]. Although it seems ORF10 has no essential functions [7], there are still some clues for us to reevaluate the significance of ORF10 function. Studies in HeLa cells found ORF10 binds and degrades mitochondrial antiviral signaling protein (MAVS) by inducing mitophagy, leading to the inhibition of antiviral innate immune response [8]. Several mutations located at *ORF10* may confer increasing pathogenesis and transmissibility to these mutant strains [9–12]. So the exact function of ORF10 may still need to be explored [13], and elaboration of ORF10-ZYG11B interaction could provide new ideas for the development of therapies for COVID-19.

ZYG11B, together with ZER1, serve as substrate receptors in the recently identified Gly/N-degron pathway [6]. Previously, we have elucidated the recognition mechanism of Gly/N-degron by ZYG11B and ZER1, and also uncovered the preference of the residues following the N-terminal glycine [14], verified that a bulky or aromatic residue following glycine is preferred by ZYG11B [6]. As the amino acids following the initiator methionine are glycine and tyrosine in ORF10, and initiator methionine followed by a small residue is constitutively cleaved by methionine aminopeptidases (MetAPs) [15], making the N-terminus of ORF10 a perfect Gly/N-degron that can be efficiently recognized by ZYG11B, which is in

* Corresponding author.
** Corresponding author.
E-mail addresses: dongcheng@tmu.edu.cn (C. Dong), xjyan@tmu.edu.cn (X. Yan).
[1] These authors contributed equally.

https://doi.org/10.1016/j.bbrc.2022.05.069
0006-291X/

agreement with previous studies. Here we report the crystal structure of ZYG11B bound to N-terminal peptide of ORF10. Our work not only unveils the recognition mechanism of ORF10 by ZYG11B, but may also shed light on further investigating the functional potential of ORF10-ZYG11B interaction as well as developing novel treatment for COVID-19.

2. Methods

2.1. Co-immunoprecipitation (Co-IP)

The gene coding for human ZYG11B (full length) was amplified from cDNA and ligated into pCDH-puro with an N-terminal Flag tag. The codon-optimized sequence encoding ORF10 was synthesized and ligated into pCDH-Ub-GPS vector (pCDH-Ub-MCS-GFP-IRES-RFP) using the seamless cloning method. The N-terminal glycine of ORF10 would be exposed by endogenous deubiquitinating enzymes (DUB) cleavage, forming an ORF10-GFP fusion protein. Human embryonic kidney (HEK293) cells were co-transfected with pCDH-Flag-ZYG11B and pCDH-Ub-ORF10-GFP-IRES-RFP plasmids using the polyethyleneimine (PEI) reagent. HEK293 cells co-transfected with pCDH-Ub-ORF10-GFP-IRES-RFP and pCDH Vector, pCDH-Ub-NIP3A-GFP-IRES-RFP and pCDH Vector, as well as pCDH-Ub-NIP3A-GFP-IRES-RFP and pCDH-Flag-ZYG11B were used as controls. Two days after transfection, cells were collected and lysed by sonication in lysis buffer [50 mM Tris-HCl pH 7.4, 250 mM NaCl, 0.5% Triton X100, 10% glycerol, 1 mM DTT, 1 × complete protease inhibitor cocktail (Roche)] on ice and sequentially centrifuged at 21,000×*g* for 20 min. The supernatants were incubated with anti-GFP affinity gel (ABclonal) at 4 °C overnight. After washes 5 times with lysis buffer, co-immune complexes were subjected to western blotting with corresponding antibodies.

2.2. Cloning, protein expression and purification

The gene coding for human ZYG11B (residues 485–728) was amplified from cDNA and the coding sequence of Tyr-Ile-Asn-Val-Gly (YINVG) was appended to its 5' end. The fusion DNA fragment was cloned into pET28-MKH8SUMO vector (Addgene Plasmid #79526) using seamless cloning method. The recombinant plasmid was transformed into *E. coli* BL21 (DE3) with Kanamycin selection, and the fusion protein expression was induced by addition of 0.2 mM isopropyl β-D-1-thiogalactopyranoside (IPTG) at 18 °C overnight. Cells were harvested by centrifugation (6000 rpm, 10 min, 4 °C), suspended with lysis buffer [20 mM Tris-HCl (pH 7.5), 400 mM NaCl] and lysed by sonication on ice. The supernatant was obtained by centrifugation (14000 rpm, 40 min, 4 °C) and collected to incubate with Ni-NTA beads. After rinsing by 25 mM imidazole in lysis buffer, the fusion protein was eluted with 250 mM imidazole in lysis buffer. The SUMO tag was cleaved by TEV protease in lysis buffer and removed by passing through a Ni-NTA column. Further purification was performed by anion exchange chromatography (HiTrap Q HP column, GE healthcare) followed by size exclusion chromatography (SEC) (Superdex 200 10/300 GL, GE healthcare) pre-equilibrated with gel-filtration buffer (20 mM Tris-HCl pH 7.5, 150 mM NaCl and 1 mM DTT). The purified protein was concentrated to about 10 mg ml^{-1}, flash frozen in liquid nitrogen and stored at −80 °C for later use.

2.3. Protein crystallization

Crystallization trials were performed using the sitting-drop vapor diffusion technique at 18 °C by mixing 1 μl protein solution (10 mg ml^{-1}) with an equal volume of reservoir solution. Crystals were obtained under condition of 0.1 M MES pH 6.5, 1.6 M $MgSO_4$. Crystals were transferred into a cryoprotectant containing 85% crystallization solution and 20% glycerol, picked up in a nylon loop and flash-frozen in liquid nitrogen.

2.4. Data collection and processing

Diffraction data were collected on the beamline BL02U at Shanghai Synchrotron Radiation Facility (SSRF) and processed with XDS [16]. The structure was solved by molecular replacement with Phaser [17] using PDB entry 7EP1 structure as a search template. The structural model was further optimized by manual building in Coot [18] and refining using PHENIX.Refine [19].

3. Results

3.1. The overall structure of ORF10 N-terminal peptide bound to ZYG11B

To confirm the interaction between ORF10 and ZYG11B, we performed Co-IP by HEK293 cells co-expressing Flag-ZYG11B and full-length ORF10-GFP, and found ZYG11B interacts with full-length ORF10 in our experiment system (Fig. 1A). In previous studies, we have already shown ARM (armadillo) repeats of ARM3-8 in ZYG11B are responsible for binding with Gly/N-degrons [14]. And ZYG11B has been shown to specifically recognize the N-terminus of ORF10 [5]. To explore this binding mechanism by determining the complex structure, we adopted the same technique as we used to solve the complex structures of ZYG11B bound to Gly/N-degrons [14]. We fused the N-terminal peptide of ORF10 (GYINVG) to the N-terminus of $ZYG11B_{485-728}$, and TEV protease cleavage exposes the glycine in the N-terminus of the fusion protein (Fig. 1B). During the purification process of the fusion protein, we found it was eluted between thyroglobulin (Mr, 67 kDa) and β-lactoglobulin (Mr, 35 kDa) in SEC (size exclusion chromatography), indicating this fusion protein exists as a dimer in solution (Fig. S1). Then, we successfully obtained crystals of this fusion protein, and determined the crystal structure at a 2.6 Å resolution (Table 1). Consistent with the SEC result, there are two protein molecules in one asymmetric unit forming a dimer by binding with the N-terminus of each other (Fig. 1C).

In the dimeric structure, each monomer presents the complex structure of ZYG11B (ARM3-8) bound to an ORF10 peptide (GYINVG). These two complex structures are almost identical with a root-mean-square deviation (r.m.s.d.) of 0.36 Å over 221 Cα atoms (Fig. 1D). Most of ZYG11B residues and all ORF10 residues are visible in the structure. The overall structure of $ZYG11B_{485-728}$ bound to ORF10 peptide is similar to that of the other degron-bound ones, which exhibits an arch-shaped conformation consisting of six ARM repeats (ARM3-8) with ORF10 peptide located in the center (Fig. 1D). A canonical ARM repeat contains three helices (H1, H2, and H3). H2 and H3 pack against one another in an antiparallel form and H1 usually lies perpendicular to the hairpin formed by the two longer helices of H2 and H3 [20].The conformation variation of ARM6-H3 helix and ARM7-H1 helix of ZYG11B to an elongated loop in this structure is also identical to other degron-bound ZYG11B structures. As a result, ZYG11B utilizes its conserved degron binding pocket to accommodate ORF10 N-terminus (Fig. 2A).

3.2. The recognition mechanism of ORF10 N-terminus by ZYG11B

Through analysis of the complex structure of ZYG11B bound to ORF10 peptide, we found that ZYG11B recognizes the N-terminus of ORF10 in a similar fashion to that of other Gly/N-degrons. In the deep degron binding cavity of ZYG11B, N-terminal glycine (G1) of ORF10 peptide is deeply buried in the narrow, negative charged

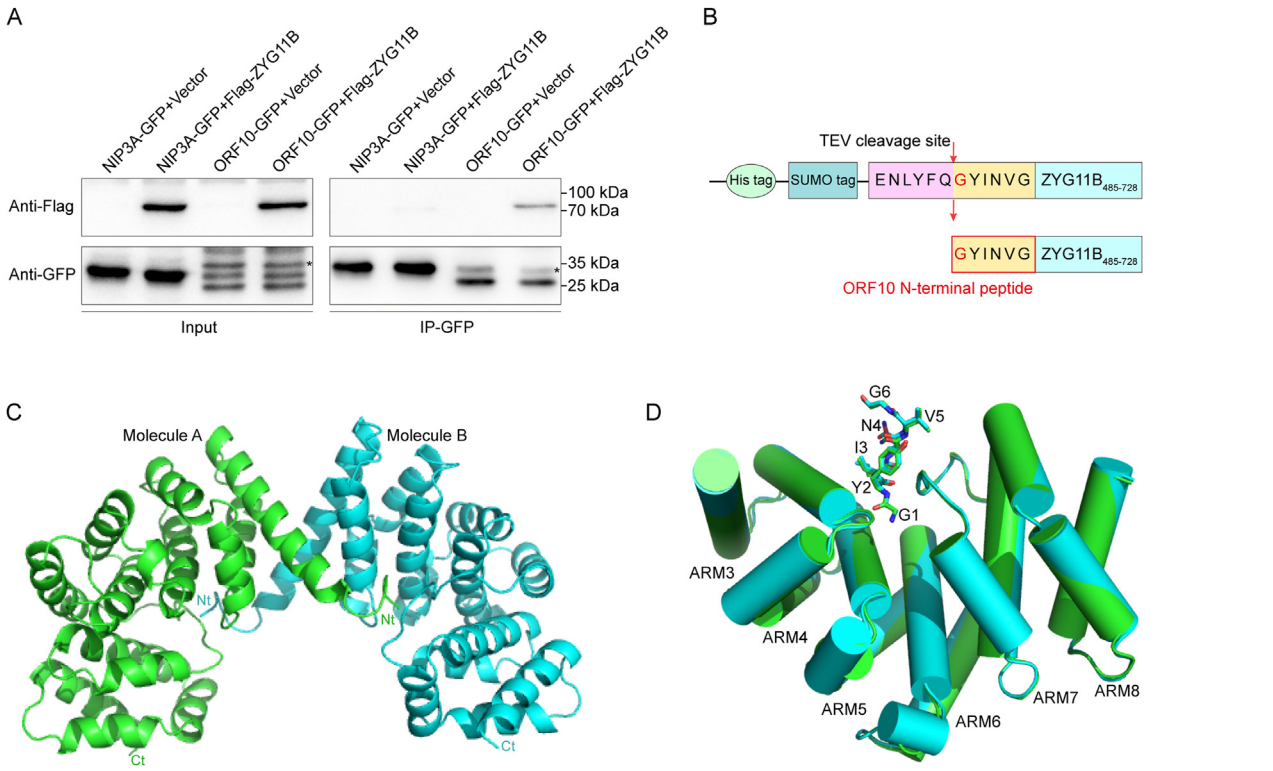

Fig. 1. Crystal structure of ZYG11B bound to N-terminus of ORF10 (A) Co-IP of Flag-ZYG11B with ORF10−GFP. NIP3A−GFP was co-expressed with Flag-ZYG11B or empty vector control. ORF10−GFP was co-expressed with Flag-ZYG11B or empty vector control. Cellular lysates and GFP gel-bound precipitates were immunoblotted as indicated. Asterisks denote ORF10-GFP bands. (B) Schematic of the recombinant construct used for the crystallization assay. The ORF10 N-terminal peptide was fused to the N-terminus of ZYG11B and was exposed by TEV protease cleavage during purification. (C) Ribbon diagram of the crystal structure of ZYG11B$_{485-728}$ bound to N-terminus of ORF10, which forms a dimer. (D) Superposition of the molecule A (green) and molecule B (cyan) in dimeric structure of ZYG11B$_{485-728}$ bound to ORF10 peptide. ORF10 peptide (GYINVG) is shown as sticks, and ARM3−ARM8 are shown as cylinders. (For interpretation of the references to colour in this figure legend, the reader is referred to the Web version of this article.)

Table 1
Data collection and refinement statistics.

	GYINVG-ZYG11B$_{485-728}$
Data collection	
Space group Cell dimensions	P 2_12_12
a, *b*, *c* (Å)	52.50, 96.85, 121.75
α, *β*, *γ* (°)	90, 90, 90
Resolution (Å)	37.26−2.60 (2.69−2.60)
R_{merge}	0.056 (0.968)
$I/\sigma I$	31.83 (4.37)
Completeness (%)	98.11 (97.39)
Redundancy	13.1 (13.3)
Refinement	
Resolution (Å)	37.26−2.60
No. reflections	19500 (1905)
R_{work}/R_{free}	0.1883/0.2696
No. atoms	
Protein	3945
Ligand	10
Water	30
B-factors	
Protein	70.81
Ligand	86.94
Water	50.18
R.m.s. deviations	
Bond lengths (Å)	0.009
Bond angles (°)	1.06
Ramachandran Plot favored/allowed/outliers (%)	97.12/2.88/0

pocket at the bottom of the cavity (Fig. 2A). Y2 perfectly fits into the inverted L-shaped pocket, with its side chain extending into the large hydrophobic groove. I3 and N4 sit near the entrance of the cavity, while V5 and G6 are exposed to solvent, thus making minor contribution to ORF10 peptide recognition.

Besides the perfectly fitted binding cavity, ZYG11B recognizes ORF10 peptide through multiple intermolecular interactions (Fig. 2B). The α-amino group of G1 is hydrogen bonded to Asp526 and Asn567 of ZYG11B as well as a water molecule which also forms hydrogen bond with Glu570. The α-carbonyl group of G1 forms two hydrogen bonds with Asn567 and Trp522 of ZYG11B. As a result, G1 forms five conserved hydrogen bonds with ZYG11B making it determinant for ORF10 recognition. Y2 forms T-shaped π-π and backbone-π stacking interaction with the indole group of Trp522 in ZYG11B. Moreover, Y2 also forms two main chain hydrogen bonds with Ala647 in ZYG11B. I3 is hydrogen bonded to Asn523 in ZYG11B with its backbone amide, and makes hydrophobic interaction with Trp522 in ZYG11B. Taken together, the first three residues in ORF10 predominantly mediate its recognition by ZYG11B through multiple intermolecular interactions.

3.3. Comparison of the ORF10 N-terminus recognition with that of one Gly/N-degron

We compared the ZYG11B-ORF10 peptide structure with that of ZYG11B-ZNF701 peptide, one of Gly/N-degron bound complex structures. Superposition of the two ZYG11B complexes reveals that they are almost identical to a r.m.s.d. of 0.28 Å over 224 Cα atoms (Fig. 3). The conformation and interaction mode are just the same between ORF10 and ZNF701 peptides, although they differ in sequence (Fig. 3). Collectively, the structure of ZYG11B bound to ORF10 peptide not only supports the recognition preference of ZYG11B no matter whether its binding partner serves as a substrate

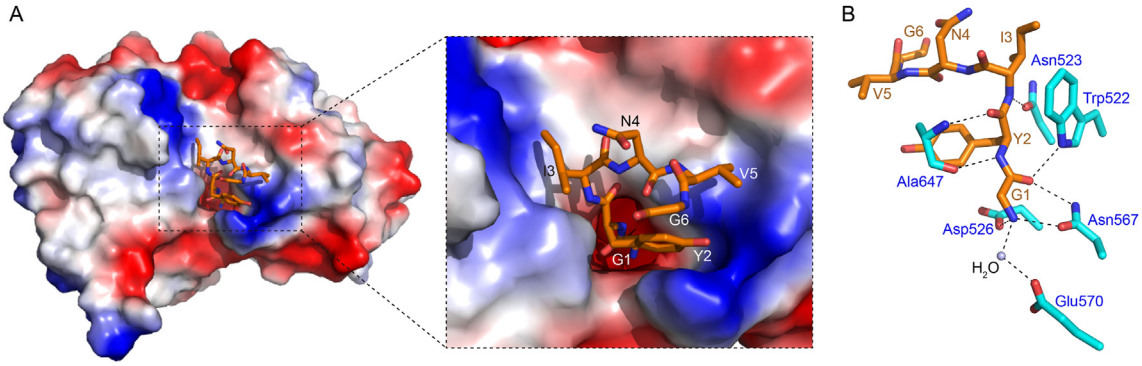

Fig. 2. Characterization of N-terminus of ORF10 recognition by ZYG11B (A) Top view of the ORF10 peptide-binding pocket of ZYG11B. $ZYG11B_{485-728}$ is shown as an electrostatic potential surface (red, negative; blue, positive). The degron is shown as orange sticks. (B) Interactions of ZYG11B with the ORF10 peptide. The peptide is shown as orange sticks, the interacting residues in ZYG11B are shown as cyan sticks, the water molecule is shown as a light blue sphere, and the hydrogen bonds are shown as black dashed lines. (For interpretation of the references to colour in this figure legend, the reader is referred to the Web version of this article.)

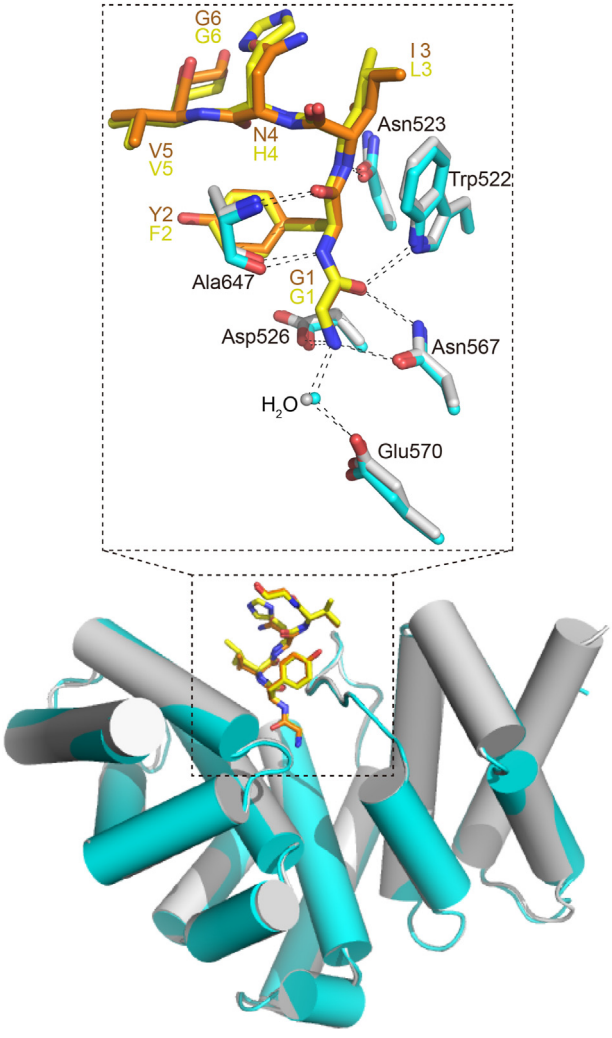

Fig. 3. Comparison of the N-terminus of ORF10 recognition with that for the SNX701 N-degron. Structure of ZYG11B (cyan)-ORF10 (orange) is superimposed with that of ZYG11B (gray)-SNX701 (yellow). ^{1}GYINVG^{6} of ORF10 and ^{1}GFLHVG^{6} of SNX701 are shown as orange and yellow sticks, respectively. ZYG11B residues involved in recognizing the GYINVG and GFLHVG motifs are shown as cyan and gray sticks, respectively. Water molecules forming hydrogen bonds with GYINVG and GFLHVG motifs are shown as cyan and gray spheres, respectively. (For interpretation of the references to colour in this figure legend, the reader is referred to the Web version of this article.)

or not, but also provides clue to explore functions of ZYG11B beyond mediation of protein degradation.

4. Discussion

N-degron pathway is the first identified pathway for short-lived proteins targeted by proteasomal degradation [21]. But it took a long time for people to discover Gly/N-degron pathway, because metazoan proteomes lack Gly/N-degron to avoid targeting by ZYG11B and ZER1, so as to maintain proteome stability [6]. So Gly/N-degrons usually present after proteolytic cleavage or in protozoan proteomes. Gly/N-degron pathway may participate in apoptosis through degradation of caspase-cleaved products [6]. The autoinhibitory NLRP1 N-terminal fragment can also be targeted by Gly/N-degron pathway after enteroviral 3C protease cleavage, thus activating the human NLRP1 inflammasome in airway epithelia [22], suggesting ZYG11B and ZER1 may be essential in immune response. SARS-CoV-2 as a protozoan, its genome encodes a putative protein ORF10 which shows a strong interaction with ZYG11B. ORF10 is relevant to the inhibition of antiviral innate immune response [8], and may contribute to pathogenesis and transmissibility of SARS-CoV-2 [9–12], indicating its interaction with ZYG11B could probably modulate immune response, thus varying the pathogenesis and transmissibility of SARS-CoV-2. Therefore, our work not only elucidates the recognition mechanism of ORF10 by ZYG11B, but may also inspire further investigation on the functional potential of ORF10-ZYG11B interaction and facilitate the development of novel therapies for COVID-19.

Accession numbers

The coordinates and structure factor files of the GYINVG-ZYG11B485-728 was deposited into Protein Data Bank (www.rcsb.org), with the accession number 7XV7.

Declaration of competing interest

The authors declare that they have no competing economic interests or personal relationships that affect the work of this article.

Acknowledgments

We thank the staff at beamline BL02U of the Shanghai Synchrotron Radiation Facility. This work was supported by the National Natural Science Foundation of China grants 31900865 (to C.D.), 32071193 (to C.D.), and 81874039 (to X.Y.).

Appendix A. Supplementary data

Supplementary data to this article can be found online at https://doi.org/10.1016/j.bbrc.2022.05.069.

References

[1] L.R. Wong, S. Perlman, Immune dysregulation and immunopathology induced by SARS-CoV-2 and related coronaviruses - are we our own worst enemy? Nat. Rev. Immunol. 22 (2022) 47–56.
[2] C. Wang, P.W. Horby, F.G. Hayden, et al., A novel coronavirus outbreak of global health concern, Lancet 395 (2020) 470–473.
[3] C.X. Li, J. Gao, Z. Zhang, et al., Multiomics integration-based molecular characterizations of COVID-19, Briefings Bioinf. 23 (2022) 1–17.
[4] D.E. Gordon, G.M. Jang, M. Bouhaddou, et al., A SARS-CoV-2 protein interaction map reveals targets for drug repurposing, Nature 583 (2020) 459–468.
[5] E.A.-O. Mena, C.A.-O. Donahue, L.P. Vaites, et al., ORF10-Cullin-2-ZYG11B complex is not required for SARS-CoV-2 infection, Proc. Natl. Acad. Sci. Unit. States Am. 118 (2021), e2023157118.
[6] R.T. Timms, Z. Zhang, D.Y. Rhee, et al., A glycine-specific N-degron pathway mediates the quality control of protein N-myristoylation, Science 365 (2019), eaaw4912.
[7] K.A.-O. Pancer, A.A.-O. Milewska, K.A.-O. Owczarek, et al., The SARS-CoV-2 ORF10 is not essential in vitro or in vivo in humans, PLoS Pathog. 16 (2020), e1008959.
[8] X. Li, P. Hou, W. Ma, et al., SARS-CoV-2 ORF10 suppresses the antiviral innate immune response by degrading MAVS through mitophagy, Cell. Mol. Immunol. 19 (2022) 67–78.
[9] S.S. Hassan, K. Lundstrom, Á. Serrano-Aroca, et al., Emergence of unique SARS-CoV-2 ORF10 variants and their impact on protein structure and function, Int. J. Biol. Macromol. (2022) 128–143.
[10] Y. Wang, D. Chen, C. Zhu, et al., Genetic surveillance of five SARS-CoV-2 clinical samples in Henan province using nanopore sequencing, Front. Immunol. 13 (2022), 814806.
[11] N. Redondo, S. Zaldivar-Lopez, J.J. Garrido, et al., SARS-CoV-2 accessory proteins in viral pathogenesis: knowns and unknowns, Front. Immunol. 12 (2021), 708264.
[12] D.M. Yang, F.C. Lin, P.H. Tsai, et al., Pandemic analysis of infection and death correlated with genomic open reading frame 10 mutation in severe acute respiratory syndrome coronavirus 2 victims, J. Chin. Med. Assoc. 84 (2021) 478–484.
[13] M.E.A. Mohammed, SARS-CoV-2 proteins: are they useful as targets for COVID-19 drugs and vaccines? Curr. Mol. Med. 22 (2022) 50–66.
[14] X. Yan, Y. Li, G. Wang, et al., Molecular basis for recognition of Gly/N-degrons by CRL2(ZYG11B) and CRL2(ZER1), Mol. Cell 81 (2021) 3262–3274, e3263.
[15] R.A. Bradshaw, W.W. Brickey, K.W. Walker, N-terminal processing: the methionine aminopeptidase and N alpha-acetyl transferase families, Trends Biochem. Sci. 23 (1998) 263–267.
[16] W. Kabsch, Xds, Acta Crystallogr. Sect. D Biol. Crystallogr. 66 (2010) 125–132.
[17] A.J. McCoy, R.W. Grosse-Kunstleve, P.D. Adams, et al., Phaser crystallographic software, J. Appl. Crystallogr. 40 (2007) 658–674.
[18] P. Emsley, K. Cowtan, Coot: model-building tools for molecular graphics, Acta Crystallogr. Sect. D Biol. Crystallogr. 60 (2004) 2126–2132.
[19] P.D. Adams, R.W. Grosse-Kunstleve, L.W. Hung, et al., PHENIX: building new software for automated crystallographic structure determination, Acta Crystallogr. Sect. D Biol. Crystallogr. 58 (2002) 1948–1954.
[20] A.H. Huber, W.J. Nelson, W.I. Weis, Three-dimensional structure of the armadillo repeat region of beta-catenin, Cell 90 (1997) 871–882.
[21] A. Bachmair, D. Finley, A. Varshavsky, In vivo half-life of a protein is a function of its amino-terminal residue, Science 234 (1986) 179–186.
[22] K.S. Robinson, D.E.T. Teo, K.S. Tan, et al., Enteroviral 3C protease activates the human NLRP1 inflammasome in airway epithelia, Science 370 (2020) eaay2002.